

Complex Langevin Lattice QCD for Color-Superconductivity at Extremely High Density

Kohtaroh Miura

KEK, Institute of Particle and Nuclear Studies, Theory Center

2024 December 11 at KEK-THEORY Workshop

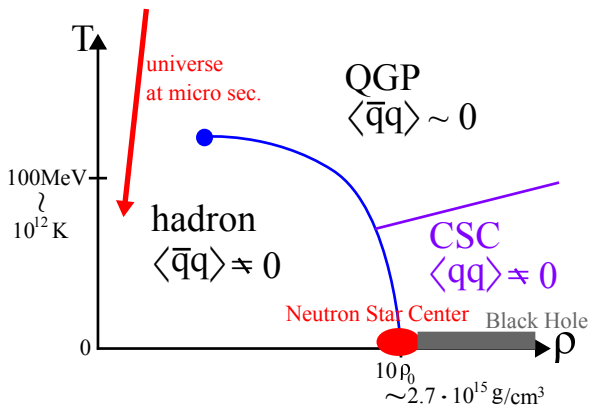
Collaboration

Yuhma Asano	(University of Tsukuba)
Yuta Ito	(Tokuyama College)
Hideo Matsufuru	(KEK/SOKENDAI)
Kohtaroh Miura	(KEK-IPNS)
Yusuke Namekawa	(Hiroshima University)
Jun Nishimura	(KEK/SOKENDAI)
Asato Tsuchiya	(Shizuoka University)
Shoichiro Tsutsui	(RIKEN-iTHEMS)
Takeru Yokota	(RIKEN)

References

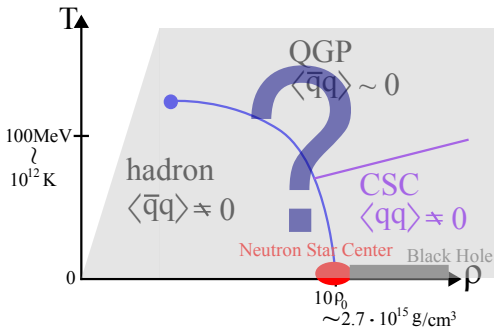
- [1] T. Yokota, Y. Ito, H. Matsufuru, Y. Namekawa, J. Nishimura, A. Tsuchiya and S. Tsutsui, JHEP **06** (2023), 061 [arXiv:2302.11273 [hep-lat]].
- [2] S. Tsutsui, Y. Asano, Y. Ito, H. Matsufuru, Y. Namekawa, J. Nishimura, A. Tsuchiya and T. Yokota, PoS **LATTICE2021**, 533 (2022) [arXiv: 2111.15095 [hep-lat]].
- [3] Y. Ito, H. Matsufuru, Y. Namekawa, J. Nishimura, S. Shimasaki, A. Tsuchiya and S. Tsutsui, JHEP **10**, 144 (2020) [arXiv: 2007.08778 [hep-lat]].

QCD Phase Diagram



The QCD phase diagram is very interesting.

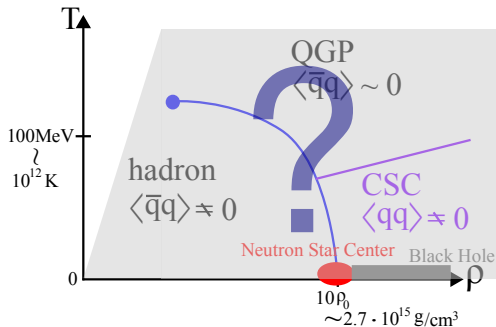
QCD Phase Diagram



High ρ : First principle calculations are very limited

due to **Sign Problem** in Monte Carlo based LQCDs.

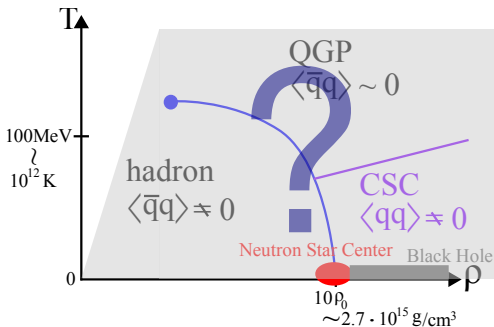
QCD Phase Diagram



High ρ : **Colorsuperconductor (CSC)**, [4]- [7]) or Quarkyonic [9, 10]?

[4] Barrois (NPB'77), [5] Frautschi (SpringerUSA'80), [6] Bailin et al (NPB'81), [7] Alford et al (PLB'98), [9] McLerran et al (NPA'07), [10] Hidaka et al (NPA'08).

QCD Phase Diagram



High ρ : Attack the sign problem by
Complex Langevin based LQCD (CL-LQCD) for CSC.

c.f. Lefschetz Thimble, TRG, LYZ, Quantum Computer...

Small-Box QCD with Gap Equation

T. Yokota et al, JHEP'23. [1]:

Small-Box QCD (on **Lattice**) $L_s < \Lambda_{QCD}^{-1} \sim$ One-Loop QCD Gap Eq.Dyson eq.
in Nambu basis

$$\Sigma = S^{-1} - S_{\text{free}}^{-1}$$

Emerged by $\Sigma_{12(21)}$

$$S = \begin{pmatrix} \langle \psi \bar{\psi} \rangle & \langle \psi \psi \rangle \\ \langle \bar{\psi} \bar{\psi} \rangle & \langle \bar{\psi} \psi \rangle \end{pmatrix}$$

Gap eq.
in lowest order

$$\Sigma_{12}(qaa') = \text{diagram}$$

q : momentum
 a, a' : internal d.o.f.

$$\Downarrow$$
 Linearize
Critical point
(Thouless criterion)

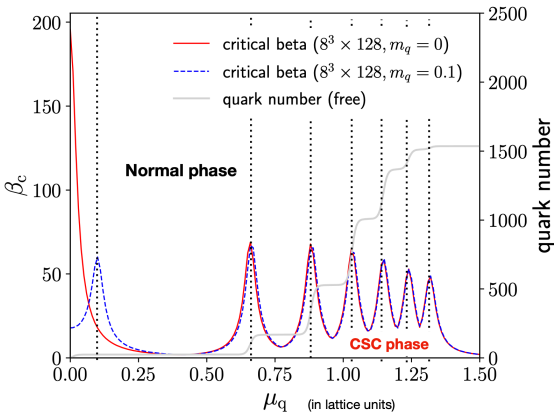
$$\frac{1}{V} \sum_{q'bb'} M_{(qaa')(q'bb')} \Sigma_{12}(q'bb') = \beta \Sigma_{12}(qaa')$$

$$\beta = 2N_c / g^2$$

- Max. eigenvalue of M
= critical lattice coupling β_c = phase boundary of normal and CSC phases.
- **No Gauge Fixing** for the diquark Σ_{12} is required.

c.f. Small-Box QCD or QCD-like models at Continuum [11, 12, 13]: S. Hands et al, JHEP'12; JHEP'10; PLB'02.

Expected Phase Diagram in Small-Box LQCD



$$E(\mathbf{q}) = \sinh^{-1} \sqrt{\sum_i \sin^2 q_i + m_q^2}$$

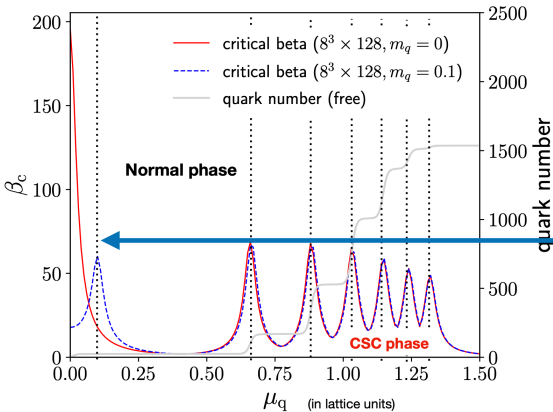
↑

$|\mathbf{q}| = 2\sqrt{2}\pi/L_s$
 $|\mathbf{q}| = 2\pi/L_s$
 $|\mathbf{q}| = 0$

Quark energy level
(discretized in finite box)

Slide borrowed from T. Yokota.

Expected Phase Diagram in Small-Box LQCD



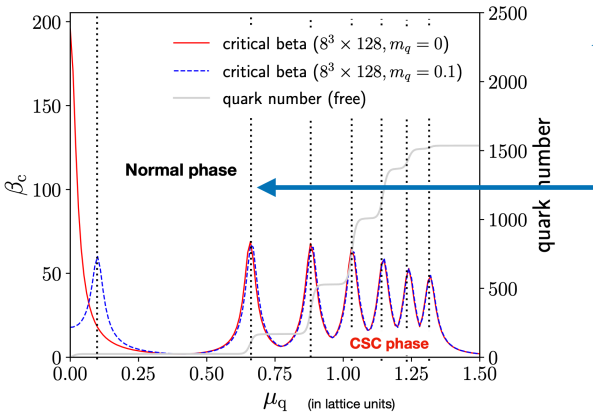
$$E(\mathbf{q}) = \sinh^{-1} \sqrt{\sum_i \sin^2 q_i + m_q^2}$$

$|\mathbf{q}| = 2\sqrt{2}\pi/L_s$
 $|\mathbf{q}| = 2\pi/L_s$
 $|\mathbf{q}| = 0$

Quark energy level
(discretized in finite box)

Slide borrowed from T. Yokota.

Expected Phase Diagram in Small-Box LQCD



$$E(\mathbf{q}) = \sinh^{-1} \sqrt{\sum_i \sin^2 q_i + m_q^2}$$

$|\mathbf{q}| = 2\sqrt{2}\pi/L_s$
 $|\mathbf{q}| = 2\pi/L_s$
 $|\mathbf{q}| = 0$

Quark energy level
(discretized in finite box)

Slide borrowed from T. Yokota.

Complex-Langevin Lattice QCD

- in a **Small-Box**,
- guided by **One-Loop QCD Gap Equations**,
- focusing on **Color superconductivity**,
- in a **gauge invariant way**.

Table of Contents

- 1 Introduction
 - QCD Phase Diagram
 - Strategy: Small-Box LQCD
- 2 Complex Langevin Method
 - Complex Langevin Method in LQCD
 - Source-Term Method
- 3 Result
 - Basic Observables
 - Response to Diquark Source-Term
- 4 Summary

Table of Contents

1

Introduction

- QCD Phase Diagram
- Strategy: Small-Box LQCD

2

Complex Langevin Method

- Complex Langevin Method in LQCD
- Source-Term Method

3

Result

- Basic Observables
- Response to Diquark Source-Term

4

Summary

Complex Langevin in Lattice QCD

Complexification of Gluon Fields:

$$U_{\mu x} \in SU(3) \implies \mathcal{U}_{\mu x}(\tau) \in SL(3, \mathbb{C}) . \quad (1)$$

Parisi '83; Klauder '84;
 Aarts, Seiler, Stamatescu '09;
 Aarts, James, Seiler, Stamatescu '11;
 Seiler, Sexty, Stamatescu '13; Sexty '14;
 Fodor, Katz, Sexty, Torok '15;
 Nishimura, Shimasaki '15;
 Nagata, Nishimura, Shimasaki '15;
 Sinclair, Kogut '16

Complex Langevin Equation:

$$\mathcal{U}_{\mu x}(\tau + \epsilon) = \exp \left[i\lambda^a \left(-\epsilon \underbrace{v_{a\mu x}[\mathcal{U}(\tau)]}_{\text{drift term}} + \sqrt{\epsilon} \underbrace{\eta_{a\mu x}(\tau)}_{\text{gaussian noise}} \right) \right] \mathcal{U}_{\mu x}(\tau) . \quad (2)$$

$$\text{c.f. For } z \in \mathbb{C}, \quad \partial_\tau z(\tau) = \underbrace{-\partial_z S(z)}_{\text{drift term}} + \underbrace{\eta(\tau)}_{\text{gaussian noise}} .$$

We expect:

$$\lim_{\tau \rightarrow \infty} \langle O[\mathcal{U}(\tau)] \rangle_\eta \stackrel{!}{=} \int DU P[U] O[U] . \quad (3)$$

Complex Langevin in Lattice QCD

For a correct convergence of Complex-Langevin processes,
(So that associated Fokker-Planck Eq. achieves correct probability distribution,)

- 1 The Drift Term,

$$v_{a\mu x}[\mathcal{U}] = \lim_{\epsilon \rightarrow 0} \frac{S[e^{i\epsilon\lambda_a} \mathcal{U}_{\mu x}] - S[\mathcal{U}_{\mu x}]}{\epsilon}, \quad (4)$$

should be regular (no singular drift problem). To confirm, monitor that the histogram of

$$v_{max} = \left(\frac{1}{\text{Vol}} \sum_{x,\mu} \sum_{i=1}^{N_c^2-1} |v_{a\mu x}|^2 \right)^{1/2}. \quad (5)$$

rapidly (exponentially) attenuates (Nagata et al, PRD'16).

- 2 The Unitarity Norm

$$\mathcal{N}_u = \frac{2}{\text{Vol}} \sum_{x\nu} \text{Tr} \left[\mathcal{U}_{x\nu}^\dagger \mathcal{U}_{x\nu} + (\mathcal{U}_{x\nu}^{-1})^\dagger \mathcal{U}_{x\nu}^{-1} - 2 \times \mathbf{1}_3 \right], \quad (6)$$

should stay small enough (no excursion of gluon fields into a deeply imaginary regime), which is achieved by a gauge cooling (Seiler et al, PLB'13).

Source-Term Method

- To extract a signal of diquark condensates on the lattice QCD, we introduce a source term

$$S_\phi = \sum_n m_\phi^2 \phi_n^{a,\dagger} \phi_{n,a} + S_J, \quad S_J = J \sum_n [\epsilon^{abc} (\chi_a \chi_b \phi_c)_n - h.c.] . \quad (7)$$

- The original staggered quark action $S_f = \bar{\chi} M \chi / 2$ is generalized as

$$S_f + S_J = \frac{1}{2} (\chi^T, \bar{\chi}) \tilde{M} \begin{pmatrix} \chi \\ \bar{\chi}^T \end{pmatrix}, \quad \tilde{M} = \begin{pmatrix} \Phi & -M^T \\ M & -\Phi^\dagger \end{pmatrix}, \quad \Phi_{nn'}^{ab} = 2J \epsilon^{abc} \phi_{n,c} \delta_{nn'} .$$

- Complex Langevin Eq. is characterized by $S_{\text{eff}} = S_G - (N_f/4) \text{Log Pf}[\tilde{M}]$.
- One might think of measuring $\langle \bar{\phi} \phi \rangle$ which is proportional to our target $\langle (\epsilon \bar{\chi} \bar{\chi}) (\epsilon \chi \chi) \rangle$. However this turns out to be too small: $\mathcal{O}(J^2)$.
- The relevant observable which we measure is the source-term itself

$$\frac{m_\phi^2}{2J} \cdot \langle \epsilon \chi \chi \phi + \epsilon \bar{\chi} \bar{\chi} \bar{\phi} \rangle, \quad (8)$$

with various J . This observable is equivalent to $\langle (\epsilon \bar{\chi} \bar{\chi}) (\epsilon \chi \chi) \rangle$, which is not straightforward to calculate (Tsutsui et al, PoS LAT2021).

Table of Contents

- 1 Introduction
 - QCD Phase Diagram
 - Strategy: Small-Box LQCD
- 2 Complex Langevin Method
 - Complex Langevin Method in LQCD
 - Source-Term Method
- 3 **Result**
 - Basic Observables
 - Response to Diquark Source-Term
- 4 Summary

Setup

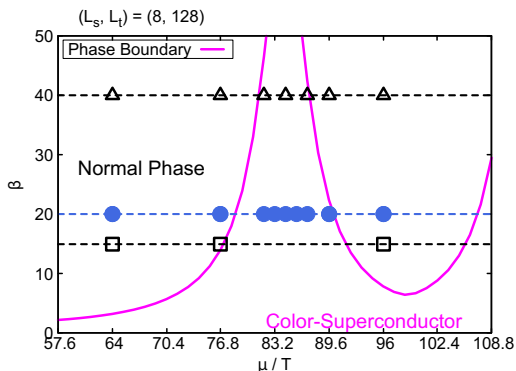
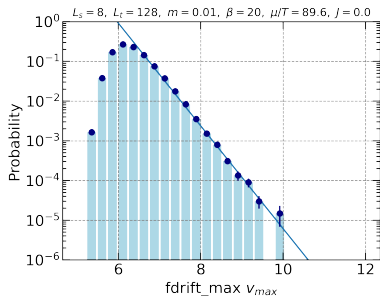
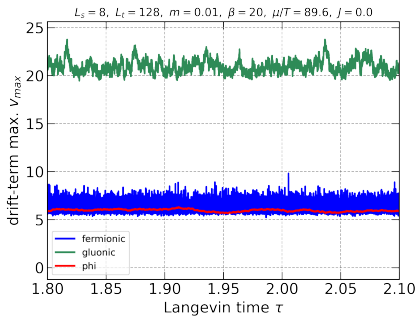


Figure:

Simulation points (blue circles) on the phase diagram predicted by the gap equation on the small-box LQCD.

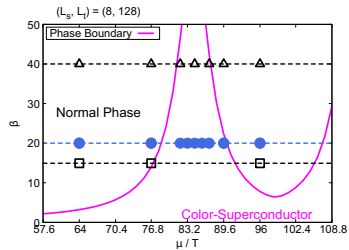
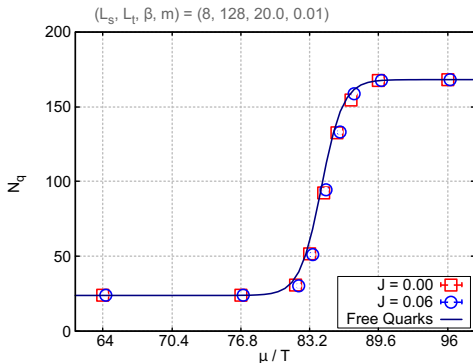
- Small-box LQCD: $(L_s, L_t, m_{lat}, \beta) = (8, 128, 0.01, 20.0)$, which realizes a cold ($L_t/L_s \gg 1$) and small-box LQCD $L_s a_{lat}(\beta) < \Lambda_{QCD}^{-1}$.
- At each simulation point, we investigate $\langle \epsilon \chi \chi \phi + h.c. \rangle$ for various J .

Example of Drift-Terms



- Left: An example of drift-terms Langevin trajectory.
- Right: A histogram for the fermion drift-term (blue trajectory in the left panel).
 - No Singular-Drift: The tail $v_{max} \geq 8$ is exponentially suppressed, $\propto e^{-3.0(2) \cdot v_{max}}$.
 - No-Excursion: $\mathcal{N}_U \sim \mathcal{O}(10^{-7})$.

Quark Number Density

Figure: Quark number density vs. quark chemical potential (T units).

Stepwise Fermi-surface: $24 \cdot 1 \rightarrow 24 \cdot (1 + 6\bar{\rho})$, where $24 = 4_{flv} \cdot 3_{col} \cdot 2_{spin}$.

Chiral Condensate

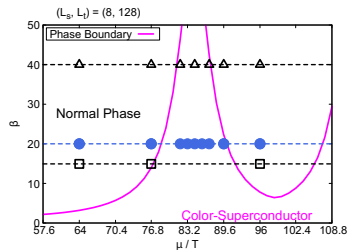
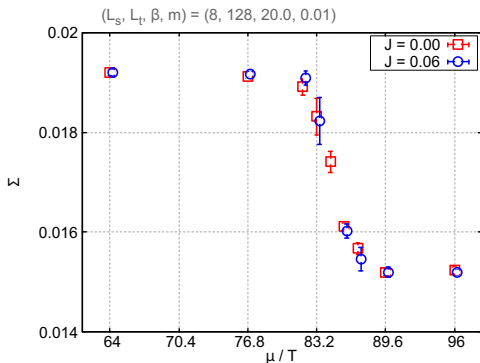


Figure: Chiral condensates vs. quark chemical potential (T units).

Chiral symmetry breaking tends to get restored with Fermi-surface formation.
(N.B. Polyakov loops stay zero-consistent.)

Diquark Source-Term: Summary

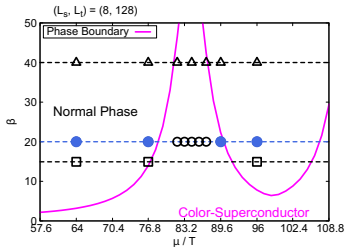
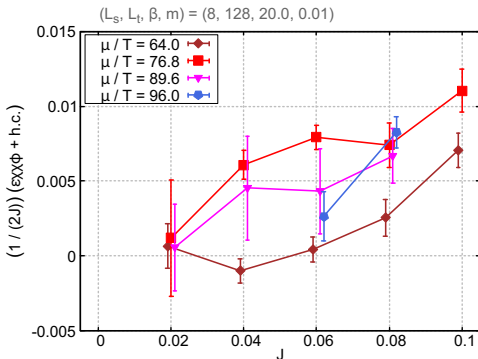


Figure: Comparison of Diquark Source Term vs. source-term coupling J .

Approaching the phase boundary from the normal phase to CSC, the response to J becomes more significant.

Diquark Source-Term: Summary

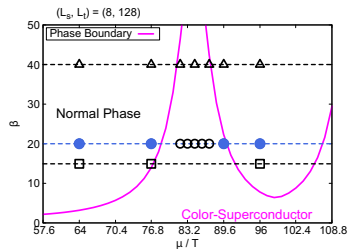
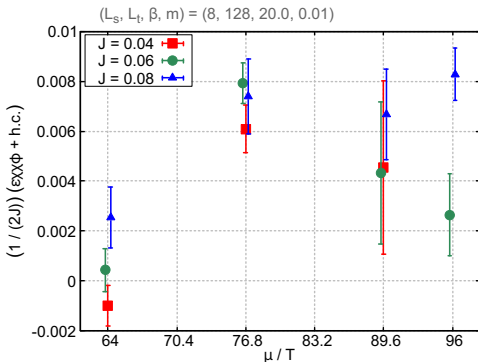


Figure: Comparison of Diquark Source Term vs quark chemical potential (T Units).

Approaching the phase boundary from the normal phase to CSC, the response to J becomes more significant.

Table of Contents

- 1 Introduction
 - QCD Phase Diagram
 - Strategy: Small-Box LQCD
- 2 Complex Langevin Method
 - Complex Langevin Method in LQCD
 - Source-Term Method
- 3 Result
 - Basic Observables
 - Response to Diquark Source-Term
- 4 Summary

Summary and Future Perspective

- We have investigated a small-box lattice QCD at high density by using the complex Langevin method.
- We have invented the diquark source-term method and investigated the color-superconductivity in a gauge-invariant way.
- Approaching the phase boundary from the normal phase, a response to the source-term coupling J becomes more significant. This implies non-linear response associated with the CSC.
- A volume dependence of the above property is under investigation:
Normal phase \implies Hadronic or Quarkyonic as $L_s a_{lat}(\beta)$ exceeds Λ_{QCD}^{-1} ?
- Ultimately, we will take (1) a infinite volume limit and then (2) $J \rightarrow 0$ limit to see whether the diquark-source term remains finite (color-superconductivity emerges).

References

- [1] T. Yokota, Y. Ito, H. Matsufuru, Y. Namekawa, J. Nishimura, A. Tsuchiya and S. Tsutsui, JHEP **06** (2023), 061 [arXiv:2302.11273 [hep-lat]].
- [2] S. Tsutsui, Y. Asano, Y. Ito, H. Matsufuru, Y. Namekawa, J. Nishimura, A. Tsuchiya and T. Yokota, PoS **LATTICE2021**, 533 (2022) [arXiv: 2111.15095 [hep-lat]].
- [3] Y. Ito, H. Matsufuru, Y. Namekawa, J. Nishimura, S. Shimasaki, A. Tsuchiya and S. Tsutsui, JHEP **10**, 144 (2020) [arXiv: 2007.08778 [hep-lat]].
- [4] B.C. Barrois, Nucl. Phys. B **129** (1977) 390.
- [5] S.C. Frautschi, Springer, U.S.A. (1980), p.19 [DOI:10.1007/978-1-4684-3602-0_2].
- [6] D. Bailin and A. Love, Nucl. Phys. B **190** (1981) 175.
- [7] M.G. Alford, K. Rajagopal, and F. Wilczek, Phys. Lett. B **422** (1998) 247 [hep-ph/9711395].
- [8] M.G. Alford, A. Schmitt, K. Rajagopal, and T. Schäfer, Rev. Mod. Phys. **80** (2008) 1455 [arXiv:0709.4635].

References

- [9] L. McLerran and R. D. Pisarski, Nucl. Phys. A **796** (2007), 83-100 [arXiv:0706.2191 [hep-ph]].
- [10] Y. Hidaka, L. D. McLerran and R. D. Pisarski, Nucl. Phys. A **808** (2008), 117-123 [arXiv:0803.0279 [hep-ph]].
- [11] S. Hands, T.J. Hollowood, and J.C. Myers, JHEP **12** (2010) 057 [arXiv:1010.0790].
- [12] S. Hands, T.J. Hollowood, and J.C. Myers, JHEP **07** (2010) 086 [arXiv:1003.5813].
- [13] S. Hands and D.N. Walters, Phys. Lett. B **548** (2002) 196 [hep-lat/0209140].

References

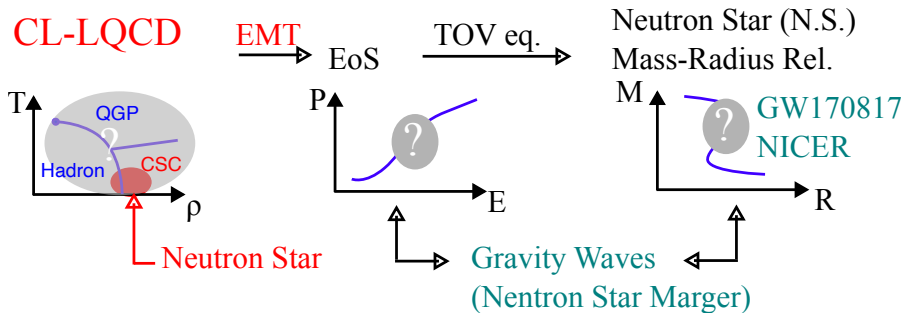
- [14] G. Parisi, Phys. Lett. B **131** (1983) 393.
- [15] J.R. Klauder, Phys. Rev. A **29** (1984) 2036.
- [16] G. Aarts, E. Seiler, and I.-O. Stamatescu, Phys. Rev. D **81** (2010) 054508 [arXiv:0912.3360].
- [17] G. Aarts, F.A. James, E. Seiler, and I.-O. Stamatescu, Eur. Phys. J. C **71** (2011) 1756 [arXiv:1101.3270].
- [18] E. Seiler, D. Sexty, and I. O. Stamatescu, Phys. Lett. B **723**, 213-216 (2013) [arXiv:1211.3709 [hep-lat]].
- [19] Z. Fodor, S.D. Katz, D. Sexty and C. Török, Phys. Rev. D **92** (2015) 094516 [arXiv:1508.05260].
- [20] K. Nagata, J. Nishimura and S. Shimasaki, PTEP **2016** (2016) no.1, 013B01 [arXiv:1508.02377 [hep-lat]].
- [21] K. Nagata, J. Nishimura, and S. Shimasaki, Phys. Rev. D **94**, no.11, 114515 (2016) [arXiv:1606.07627 [hep-lat]].
- [22] J.B. Kogut and D.K. Sinclair, Phys. Rev. D **100** (2019) 054512 [arXiv:1903.02622].

5

Backups

- Neutron Star Phenomenology

From LQCD to Neutron Star Physics



Tolman–Oppenheimer–Volkoff (TOV) Equation

- Tolman–Oppenheimer–Volkoff (TOV) Equation:

$$\frac{dP(r)}{dr} = -G \frac{(M(r) + 4\pi r^3 P(r)/c^2)(E^2 + P^2)/c^2}{r^2(1 - 2GM/(rc^2))}, \quad \frac{dM(r)}{dr} = \frac{4\pi r^2 E}{c^2}. \quad (9)$$

- TOV Eq. is a static balance condition between neutron-star pressure and gravity in general relativity: $P(r + dr) - P(r) \sim GM(r)dr/r^2$.
- When the neutron-star EoS ($P = f(E)$) is combined with TOV Eq., $M - R$ relation is extracted.

Neutron Star Structure

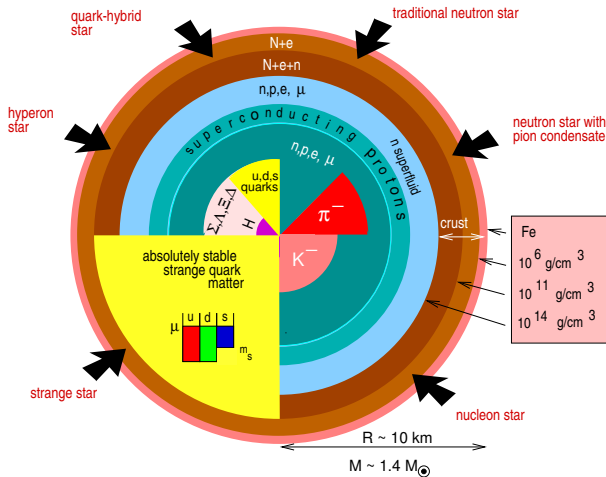


Fig: Neutron star inner structure. Quoted from [F. Weber, J. Phys. G: Nucl. Part. Phys. 27 (2001)]

Neutron Star Equation of State: Various Examples

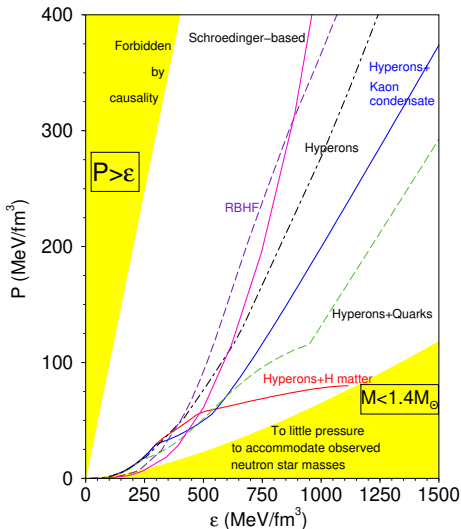


Fig: Various neutron star equation of state (EoS). Quoted from [F. Weber, J. Phys. G: Nucl. Part. Phys. 27 (2001)].

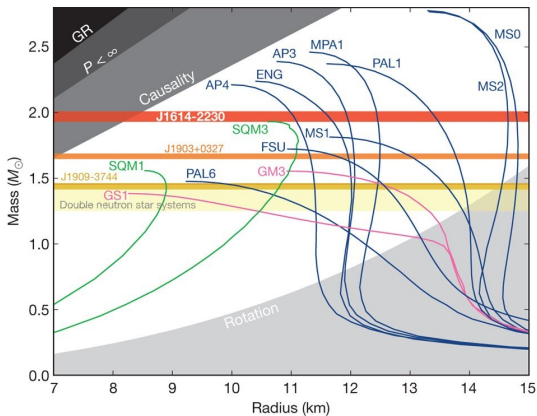
Neutron Star $M - R$ Relation

Fig: Various $M - R$ relations.

Quoted from [Nature'10, vol.467, P. Demorest et al.].